# Studying Blazars Using Fermi Gamma Ray Data

Project Report

**Dhruv Aryan**

Mentor: Professor Prajval Shastri, Raman Research Institute

Duration of Project: May, 2023 – Aug, 2023

## Introduction and Theoretical Background

### Active Galactic Nuclei

The brightness of the majority of galaxies is stellar in nature - they originate from the brightness of their constituent stars. However, some galaxies are such that their brightness originates from their extermely bright centres. These galaxies are known as Active Galaxies, and their bright centers are known as Active Galactic Nuclei (AGN). Such strong emissions from AGN have been observed in radio, microwave, infrared, optical, ultra-violet, X-ray and gamma ray bands of the energy spectrum.

Much of the physics behind AGN is unknown. AGN can therefore be seen as special laboratories for studying extreme physics. Further, they help us better understand the formation and evolution of the universe as a whole.

### Model

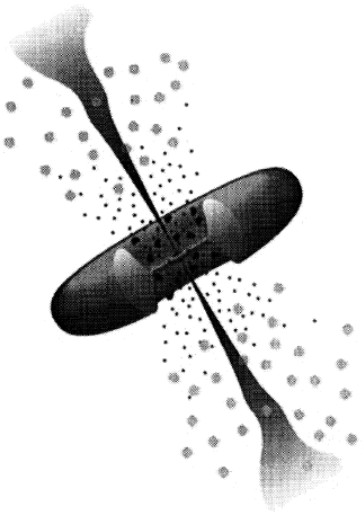

Figure 1: A schematic of the current paradigmatic model for radio-loud AGN (Urry and Padovani, 1995)

As shown in Figure 1, the largely agreed upon model for radio-loud AGN consists of a supermassive black hole at the center whose gravitational potential energy is the source of AGN luminosity. Matter approaching the black hole loses angular momentum due to turbulence in an accretion disc, emitting ultraviolet and X-ray light. Hard X-rays are generated close to the black hole, possibly linked to energetic electrons above the disk. The spin of the black hole allows the extraction of electromagnetic energy from it. Rapidly moving gas clouds emit optical and ultraviolet lines, while obscured from some angles by a torus or gas-dust disk. Slower gas clouds beyond the torus produce narrower emission lines. Energetic particles from the disk poles form radio-emitting jets, creating strong radio sources in elliptical galaxies but weaker ones in gas-rich spirals. These jets consist of plasma moving at high velocities, beaming radiation relativistically in the forward direction (Holt, Neff, and Urry, 1992).

## Classes of AGN

AGN are categorized by their radio loudness and optical emission line properties. Radio-loud AGN have high radio-to-optical flux ratios. Both radio-loud and radio-quiet AGN are further divided into Type 0, Type 1, and Type 2 based on their emission lines.

Type 1 AGN exhibit strong continua and wide emission lines due to high-velocity gas near the central black hole. This includes Seyfert 1 galaxies with lower luminosities and nearby visibility, and radio-quiet quasars (QSO) with higher luminosities seen at greater distances. These radio-quiet Type 1 AGN are subdivided into Broad-Line Radio Galaxies (BLRG) or radio-loud quasars like Steep Spectrum Radio Quasars (SSRQ) or Flat Spectrum Radio Quasars (FSRQ) based on their radio continuum shape.

Type 2 AGN have weak continua and narrow emission lines, suggesting absence of high-velocity gas or obscured line of sight. Radio-quiet Type 2 AGN include Seyfert 2 galaxies and narrow-emission-line X-ray galaxies (NELG). At higher luminosities, plausible candidates are infrared-luminous IRAS AGN with Type 2 optical spectra. Radio-loud Type 2 AGN are Narrow-Line Radio Galaxies (NLRG), with Fanaroff-Riley type I and II radio galaxies.

A subset of AGN, named Type 0, display unique spectral traits. These might be oriented at a small angle to the line of sight. This group includes radio-loud BL Lac objects without clear emission or absorption features, and about 10% of radio-quiet AGN with broad P-Cygni-like absorption features, termed BAL quasars.

Type 1 quasars like Optically Violent Variable (OVV) quasars, Highly Polarized Quasars (HPQ), Core-Dominated Quasars (CDQ), and FSRQ, resemble BL Lac objects and are possibly observed at small angles to the line of sight. These exhibit rapid variability, high polarization, and high brightness temperatures, and are consolidated as FSRQ. Both BL Lacs and FSRQs are called blazars, though FSRQs with broad emission lines are noted as Type 0 due to their blazar-like continuum.

Type 1 and 2 AGN differ by core obscuration, and radio-loud AGN classification as blazars or galaxies is based on relativistic jet alignment. These two factors—obscuration and relativistic beaming—shape the properties of radio-loud objects. Unifying high-luminosity radio galaxies with quasars requires accounting for both factors, while aligning low-luminosity radio galaxies with BL Lac objects primarily considers relativistic beaming (Urry and Padovani, 1995). The various AGN classes are summarised in the table below.

| | | Optical Emission Line Properties | | |
|---|---|---|---|---|
| | | **Type 2 (Narrow Line)** | **Type 1 (Broad Line)** | **Type 0 (Unusual)** |
| **Radio Loudness** | **Radio-quiet** | Sy 2<br>NELG<br>IR Quasar | Sy 1<br>QSO | BAL QSO |
| | **Radio-loud** | NLRG - FR I, FR II | BLRG<br>SSRQ<br>FSRQ | Blazars - BL Lacs, FSRQs |

Table 1: AGN Taxonomy (Urry and Padovani, 1995)

## Unification Schemes

Unification schemes propose that the different classes of AGN are the same type of object observed under different physical conditions. The most common of these are orientation-based models, in which the apparent differences between the classes of AGN are attributed to their differing orientations to the observer.

### Radio-Quiet Unification

For radio-quiet AGN, the unification models propose that Seyfert 1 galaxies are oriented such that we have a direct view of the nucleus, while Seyfert 2 galaxies are oriented such that we see the nucleus through an obscuring structure which prevents a direct view of the optical continuum, broad-line region or soft X-ray emission. The standard model is of a torus of obscuring material surrounding the accretion disk of the black hole at the center. It is large enough to obscure the broad-line region but not large enough to obscure the narrow-line region. There is material present outside the torus that can scatter some of the nuclear emission into our line of sight, allowing us to see the some optical and X-ray continuum, and sometimes broad emission lines. Infrared observations of Seyfert 2 nuclei also support this model.

### Radio-Loud Unification

For radio-loud AGN, the unification that is proposed is directly analogous to the Seyfert 1/2 unification. The large-scale radio structures of such AGN provide evidence in support of orientation-based unification models. In this picture, radio galaxies are radio-loud AGN which are oriented towards us such that their nuclei are obscured by a torus, while quasars are radio-loud AGN which are oriented towards us such that their nuclei are not obscured by the torus. At very small angles to the line of sight, relativistic beaming effects dominate and we see the object as a blazar.

## Blazars

Blazars are a class of AGN showcasing substantial variability and polarization in their continuous emissions over a wide range of wavelengths. These traits are commonly associated with the relativistic

beaming of energetic jets when these jets are closely aligned with our line of sight. Some quasars display blazar characteristics, and being quasars, they have radio structures that match the Fanaroff-Riley II type (Shastri et al., 2014).

In addition, there are other AGN demonstrating blazar traits but lacking strong emission lines in their optical spectra. These are termed BL Lacertids or BL Lacs in the literature. These AGN are believed to have synchrotron emissions overwhelmingly dominating their emissions across all wavelengths, including any emission lines (ibid.). The specifics of their extended radio structures are less well-defined and have been observed to exhibit both Fanaroff-Riley types and mixed structures (as seen in Kharb, Lister, and Cooper, 2010).

The underlying reason for this division within blazars remains unclear. Unlike in other subcategories of AGN where the absence of emission lines is explained by obscured toroidal material, this explanation does not apply to blazars, as their emissions are influenced by Doppler beaming, which points them close to our line of sight.

Ghisellini et al. (2009) have suggested that this division is not a strict separation but rather a gradual transition with a physical basis. They propose that the differentiation between BL Lacs and quasars is a consequence of a critical accretion rate. Below this rate, accretion becomes inefficient in terms of radiation, resulting in weak or absent broad emission lines as observed in BL Lacs. In these instances, gamma-ray photons emerge from an environment with limited radiation, leading to a more intense spectrum. Above the critical accretion rate, not only would broad emission lines become evident, but the inverse-Compton emission would mainly arise from external Compton processes, resulting in a comparatively softer gamma-ray spectrum.

Furthermore, Ghisellini et al. (2009) suggest that this interpretation aligns with the concept of unification, where Fanaroff-Riley radio galaxies of types I and II are considered the source populations for beamed BL Lacs and quasars, respectively. Nonetheless, the findings of Kharb et al. (2010) cast doubt on this interpretation.

# Data

## Fermi Large Array Telescope Data

The Fermi Gamma-ray Space Telescope is a space observatory used to perform gamma-ray astronomy observations from low Earth orbit. Its primary instrument is the Large Area Telescope (LAT), which is used by astronomers to perform all-sky surveys studying various astrophysical objects such as AGN, pulsars, and other high-energy sources, as well as dark matter.

The LAT is an imaging gamma-ray detector, detecting photons with energy ranging from 20 MeV to 300 GeV, with a field of view spanning around 20% of the sky.

In this project, two catalogs containing data taken by the Fermi LAT were used:

1. **LAT 14-year Source Catalog (4FGL-DR4)**: The LAT Collaboration has published a series of catalogs based on analyses of LAT data. The data for this catalog were taken during the period 4th August 2008 (15:43 UTC) to 2nd August 2022 (21:53 UTC), over a period of 14 years. The

catalog consists of objects which are gamma-ray emitters, with the energy range for the data in this catalog being 50 MeV to 1 TeV.

2. **Fourth LAT AGN Catalogue Data Release 3 (4LAC-DR3)**: This catalog contains AGN present in the Fermi 4FGL catalog. This is the third update to the catalog, and the data for this is derived from the Fermi 4FGL-DR3 catalog.

| AGN Type | High-latitude Sample | Clean Sample | Low-latitude Sample |
|---|---|---|---|
| FSRQ | 755 | 640 | 37 |
| BL Lac | 1379 | 1261 | 79 |
| Blazar of Unknown Type | 1208 | 945 | 285 |
| Non-blazar AGN | 65 | 50 | 6 |
| All | 3407 | 2896 | 407 |

Table 2: Census of 4LAC-DR3 sources (Ajello et al., 2020)

## Nordic Optical Telescope Data

The Nordic Optical Telescope (NOT) is a 2.5m telescope located at Roque de los Muchachos Observatory, La Palma in the Canary Islands, Spain. It records measurements in the optical and infrared regions of the spectrum. In this project, I have used R-band data recorded using this telescope (Nilsson et al., 2003).

## Data Matching

Data matching is the process of identifying the same object across catalogs and combining the data contained in each of these catalogs for that object. In this project, this was done using the software TOPCAT.

### Match Criteria

1. **Algorithm**: Sky - The Sky algorithm matches two objects if their RA and Dec values are within a certain range from each other. This range is determined by the "Max Error" parameter.
2. **Max Error**: 3.0 arcseconds

### Procedure

1. In the "Control Window", import the data tables that will be used for data matching.
2. Choose the "Pair Match" option from the "Joins" menu.
3. Choose the match criteria (the algorithm and max error).
4. Choose the imported data tables under "Table 1" and "Table 2".

5. For each table, ensure that the correct columns are chosen for the "RA columnn" and the "Dec column", with the appropriate unit (degrees, hours or radians).
6. Check the matched data table to see if the max error needs to be adjusted.
7. Save the matched data table.

## Luminosity Calculation

To calculate the luminosities of the objects in the energy band $E_1 - E_2$, we require the flux to be in the units of $\mathrm{W\,cm^{-2}}$, rather than photons $\mathrm{cm^{-2}\,s^{-1}}$ as presented in the Fermi 4FGL catalog. We use the following conversion:

$$\text{Flux } (\mathrm{W\,cm^{-2}}) = \text{Flux } (\text{photons}\,\mathrm{cm^{-2}\,s^{-1}}) \times \frac{\gamma - 1}{\gamma - 2} \times E_1 \times \frac{(E_2/E_1)^{2-\gamma} - 1}{(E_2/E_1)^{1-\gamma} - 1} \tag{1}$$

where $\gamma$ is the photon index. Now, to calculate the luminosity distance, I wrote a Python script, which is shown in the appendix. We then use the following equation to calculate the luminosity in W/Hz:

$$\text{Luminosity} = 4\pi \times \text{Flux } (\mathrm{W\,m^{-2}}) \times \text{Luminosity Distance} \tag{2}$$

Here, flux in $\mathrm{W\,m^{-2}}$ is calculated easily from flux in $\mathrm{W\,cm^{-2}}$ by simply multiplying the latter by $10^4$.

## Results

On plotting a histogram of the redshifts of BL Lacs and FSRQs, we obtain the following plot:

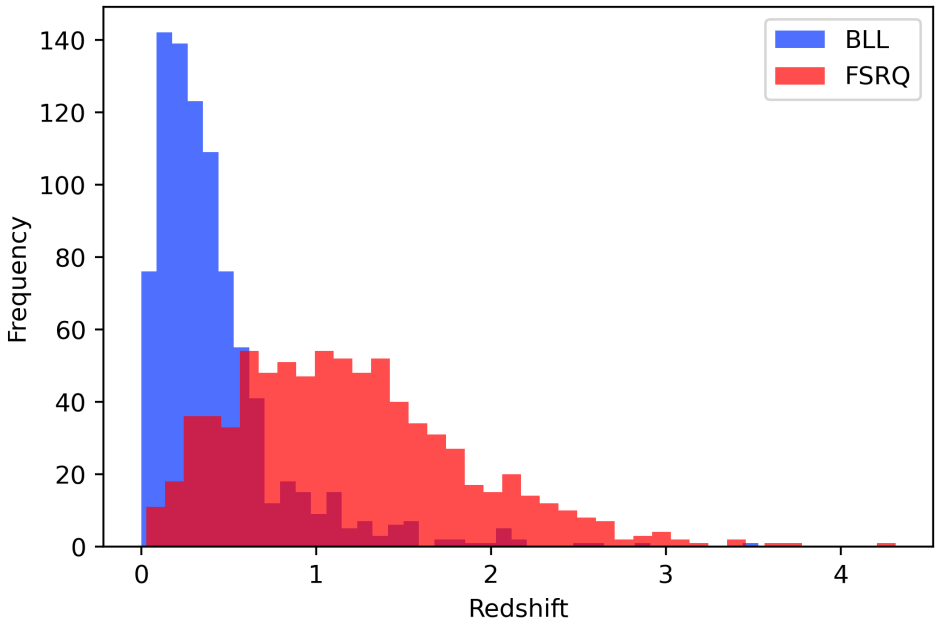


Figure 2: Histogram of redshifts of BL Lacs and FSRQs.

On calculating the luminosity of the objects using the scheme described in the previous section, we obtain luminosities for every band in the gamma part of the spectrum. On plotting the photon index against luminosity for BL Lacs and FSRQs in the 1-100 GeV band, we get the following:

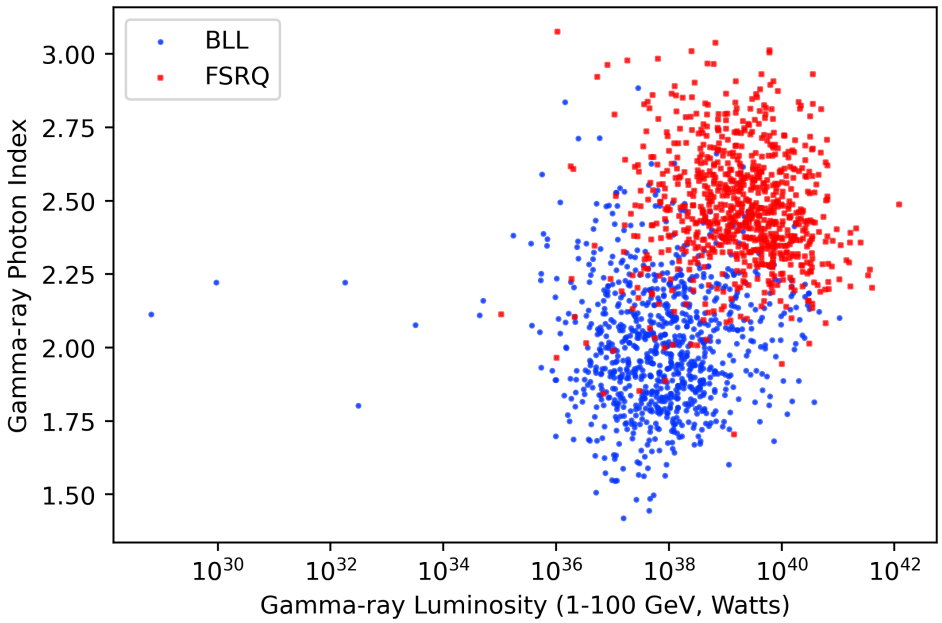


Figure 3: Plot of photon index against luminosity in the 1-100 GeV gamma ray band for BL Lacs and FSRQs.

This plot is consistent with the findings of Ghisellini, Maraschi, and Tavecchio, 2009, Ajello et al., 2020 and Shastri et al., 2014, which state that BL Lacs and FSRQs should occupy different regions in the plot. However, according to Ghisellini, Maraschi, and Tavecchio, 2009, there is a continuity between these two blazar classes. We can see that in this plot, BL Lacs and FSRQs show qualitatively different trends, which is consistent with the findings of Shastri et al., 2014. This suggests that the relationship between these two classes of blazars is one of a dichotomy rather than continuity.

On doing this plot for all bands in the Fermi data, along with plotting the luminosity in each band against the luminosity in every other band, we get the following set of plots:

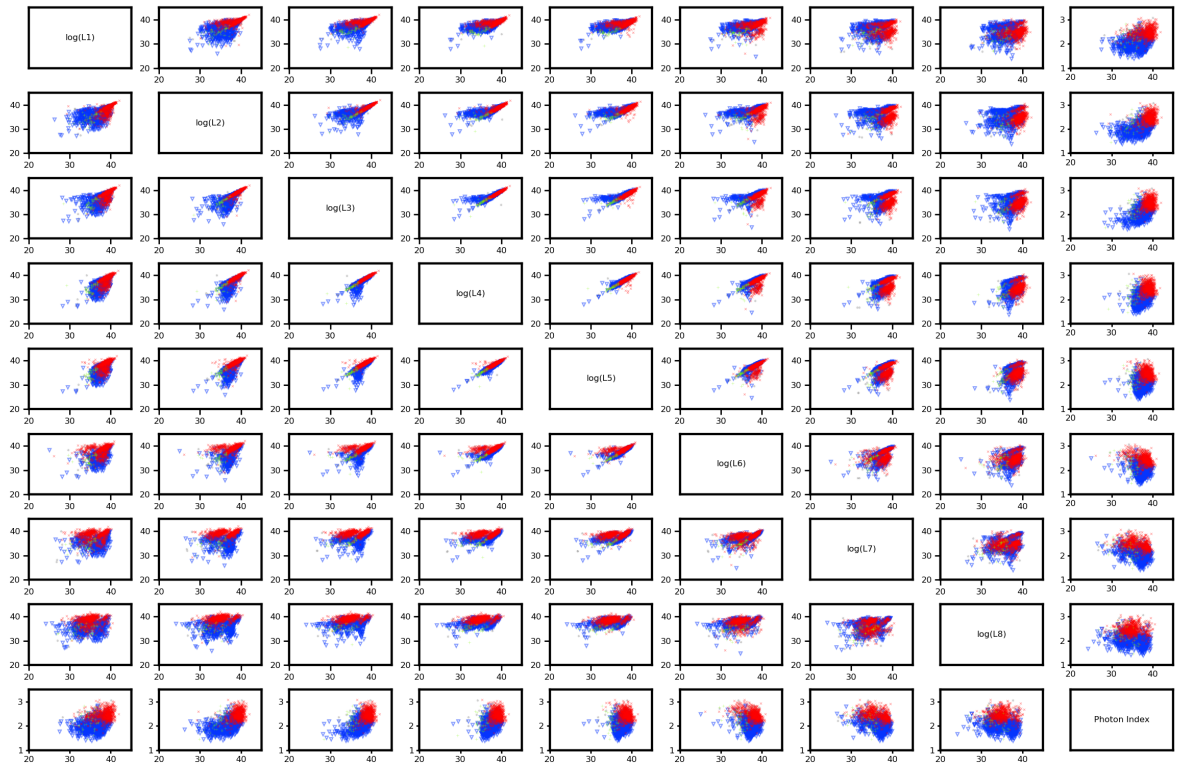


Figure 4: Plots of luminosity (in log-scale) and photon index in different Fermi gamma ray for BL Lacs and FSRQs.

The plots for eight bands in total shown in the figure above here, and these bands are as follows:

1. 50 – 100 MeV
2. 100 – 300 MeV
3. 300 – 1000 MeV
4. 1 – 3 GeV
5. 3 – 10 GeV
6. 10 – 30 GeV
7. 30 – 100 GeV
8. 100 – 1000 GeV

These bands correspond to rows 1-8 and columns 1-8 in Figure 4, with row $i$ and column $j$ filled with a plot of the luminosity in band $i$ against the luminosity in band $j$. The last row and last column are filled with plots of photon index against luminosity. In the last row, the column associated with the plot determines the energy band of the luminosity against which the photon index is plotted, and similarly, in the last column, the row associated with each plot determined the energy band of the luminosity against which the photon index is plotted. We see that in most bands, there seems to be some correlation between the luminosities in the different bands, although in some cases this is unclear, and we see that

our previous conclusions regarding the photon index-luminosity plot for the 1-100 GeV band seem to hold for all eight bands listed above.

In order to investigate the relationship between BL Lacs and FSRQs further, we need to study the Doppler factor, since relativistic aberration plays an important role in observations. To do this, we can use the radio core-dominance parameter. The radio core-dominance of an AGN is the ratio of the nuclear to lobe radio emission in the rest frame of the AGN and it is shown to be a robust statistical measure of the orientation of the radio jet axis to our line of sight (Kapahi and Saikia, 1982; Wills et al., 1992). However, due to constraints with the measurement of this parameter, we instead measure the ratio of the optical nucleus to host galaxy emission using data from the Nordic Optical Telescope (Nilsson et al., 2003), as done by Shastri et al., 2014. On plotting this luminosity in the 1-100 GeV band against this parameter, we get the following plot:

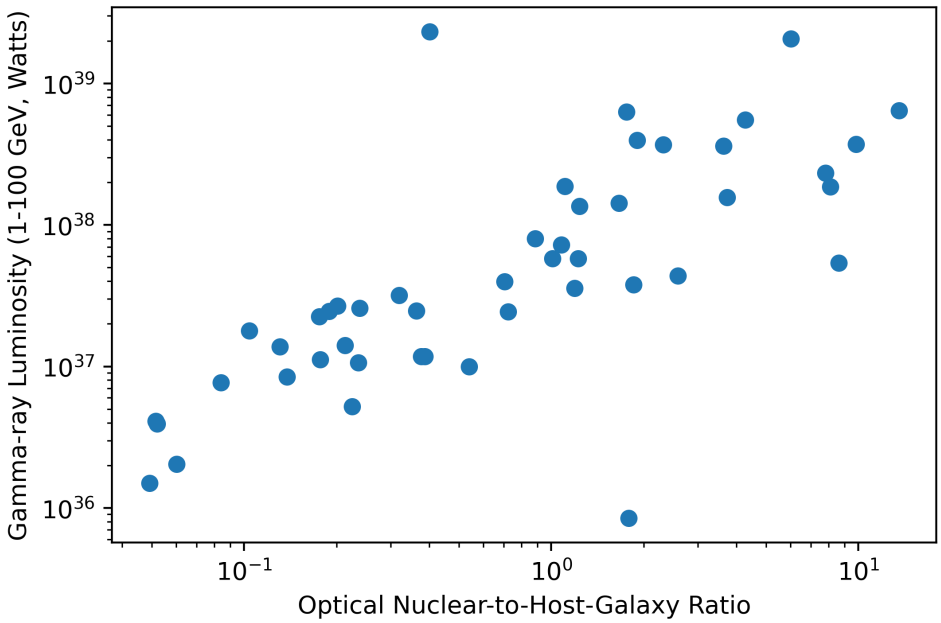


Figure 5: Plot of gamma ray luminosity against the optical nuclear-to-host-galaxy ratio.

We see an increasing linear trend in the plot shown above. This means that there is a correlation between the two quantities, which suggests that the optical nuclear-to-host-galaxy emission ratio is a good proxy for the angle to the line of sight. This makes sense since we expect the gamma ray emission to be significantly Doppler beamed, and this is consistent with the findings of ibid.

## Conclusion

The following conclusions can be drawn from this project:

1. The data suggests that the divide between BL Lacs and FSRQs is a dichotomy rather than a continuum, i.e. these seem to be physically different objects, with differing physical mechanisms underlying observed properties.

2. The ratio of the nuclear emission to the host galaxy emission in the optical part of the spectrum

seems to be a reliable parameter that can be used instead of the radio core-dominance parameter in order to measure the orientation of the radio jet with respect to our line of sight.

While we need quantitative models to investigate further, these results begin to shed some light on the properties of the blazar sub-classes and their underlying physics.

## Acknowledgments

This project made use of data from the Fermi LAT public archive. I would like to thank Professor Prajval Shastri (Astronomy and Astrophysics Department, Raman Research Institute, Bengaluru) for the opportunity to work on this project and for her guidance throughout the project. I would also like to thank Dr. Maitrayee Gupta (Institute for Research in Astrophysics and Planetology, CNRS, Toulouse) for her help and guidance.

## References

Ajello, Marco et al. (2020). "The fourth catalog of active galactic nuclei detected by the Fermi Large Area Telescope". In: *The Astrophysical Journal* 892.2, p. 105.

Ghisellini, Gabriele, L Maraschi, and F Tavecchio (2009). "The Fermi blazars' divide". In: *Monthly Notices of the Royal Astronomical Society: Letters* 396.1, pp. L105–L109.

Holt, Stephen S, Susan G Neff, and C Megan Urry (1992). "Testing the AGN paradigm: College Park, MD 1991". In: *Testing the AGN paradigm* 254.

Kapahi, VK and DJ Saikia (1982). "Relativistic beaming in the central components of double radio quasars". In: *Journal of Astrophysics and Astronomy* 3, pp. 465–483.

Kharb, P, ML Lister, and NJ Cooper (2010). "Extended radio emission in MOJAVE Blazars: Challenges to Unification". In: *The Astrophysical Journal* 710.1, p. 764.

Nilsson, K et al. (2003). "R-band imaging of the host galaxies of RGB BL Lacertae objects". In: *Astronomy & Astrophysics* 400.1, pp. 95–118.

Shastri, Prajval et al. (2014). "Systematics of jets using multi-wavelength data". In: *Proceedings of the International Astronomical Union* 10.S313, pp. 164–168.

Urry, C Megan and Paolo Padovani (1995). "Unified schemes for radio-loud active galactic nuclei". In: *Publications of the Astronomical Society of the Pacific* 107.715, p. 803.

Wills, Beverley J et al. (1992). "A survey for high optical polarization in quasars with core-dominant radio structure-Is there a beamed optical continuum?" In: *Astrophysical Journal, Part 1 (ISSN 0004-637X), vol. 398, no. 2, p. 454-475.* 398, pp. 454–475.

## Appendix

### Luminosity Calculator

```
def calc(WM,H0,z):
  WV = 1.0 - WM - 0.4165/(H0*H0)
  WR = 0.        # Omega(radiation)
  WK = 0.        # Omega curvaturve = 1-Omega(total)
```

```
  c = 299792.458 # velocity of light in km/sec
  Tyr = 977.8    # coefficent for converting 1/H into Gyr
  DTT = 0.5      # time from z to now in units of 1/H0
  DTT_Gyr = 0.0  # value of DTT in Gyr
  age = 0.5      # age of Universe in units of 1/H0
  age_Gyr = 0.0  # value of age in Gyr
  zage = 0.1     # age of Universe at redshift z in units of 1/H0
  zage_Gyr = 0.0 # value of zage in Gyr
  DCMR = 0.0     # comoving radial distance in units of c/H0
  DCMR_Mpc = 0.0
  DCMR_Gyr = 0.0
  DA = 0.0       # angular size distance
  DA_Mpc = 0.0
  DA_Gyr = 0.0
  kpc_DA = 0.0
  DL = 0.0       # luminosity distance
  DL_Mpc = 0.0
  DL_Gyr = 0.0   # DL in units of billions of light years
  V_Gpc = 0.0
  a = 1.0        # 1/(1+z), the scale factor of the Universe
  az = 0.5       # 1/(1+z(object))

  h = H0/100.
  WR = 4.165E-5/(h*h)   # includes 3 massless neutrino species, T0 = 2.72528
  WK = 1-WM-WR-WV
  az = 1.0/(1+1.0*z)
  age = 0.
  n=1000         # number of points in integrals
  for i in range(n):
    a = az*(i+0.5)/n
    adot = np.sqrt(WK+(WM/a)+(WR/(a*a))+(WV*a*a))
    age = age + 1./adot

  zage = az*age/n
  zage_Gyr = (Tyr/H0)*zage
  DTT = 0.0
  DCMR = 0.0

  # do integral over a=1/(1+z) from az to 1 in n steps, midpoint rule
  for i in range(n):
    a = az+(1-az)*(i+0.5)/n
    adot = np.sqrt(WK+(WM/a)+(WR/(a*a))+(WV*a*a))
    DTT = DTT + 1./adot
    DCMR = DCMR + 1./(a*adot)

  DTT = (1.-az)*DTT/n
  DCMR = (1.-az)*DCMR/n
  age = DTT+zage
  age_Gyr = age*(Tyr/H0)
  DTT_Gyr = (Tyr/H0)*DTT
  DCMR_Gyr = (Tyr/H0)*DCMR
  DCMR_Mpc = (c/H0)*DCMR

  # tangential comoving distance

  ratio = 1.00
  x = np.sqrt(abs(WK))*DCMR
  if x > 0.1:
    if WK > 0:
```

```
    ratio =  0.5*(exp(x)-exp(-x))/x
  else:
    ratio = sin(x)/x
else:
  y = x*x
  if WK < 0: y = -y
  ratio = 1. + y/6. + y*y/120.
DCMT = ratio*DCMR
DA = az*DCMT
DA_Mpc = (c/H0)*DA
kpc_DA = DA_Mpc/206.264806
DA_Gyr = (Tyr/H0)*DA
DL = DA/(az*az)
DL_Mpc = (c/H0)*DL
DL_Gyr = (Tyr/H0)*DL

# comoving volume computation

ratio = 1.00
x = np.sqrt(abs(WK))*DCMR
if x > 0.1:
  if WK > 0:
    ratio = (0.125*(exp(2.*x)-exp(-2.*x))-x/2.)/(x*x*x/3.)
  else:
    ratio = (x/2. - sin(2.*x)/4.)/(x*x*x/3.)
else:
  y = x*x
  if WK < 0: y = -y
  ratio = 1. + y/5. + (2./105.)*y*y
VCM = ratio*DCMR*DCMR*DCMR/3.
V_Gpc = 4.*np.pi*((0.001*c/H0)**3)*VCM

return DL_Mpc

```

Listing 1: Luminosity Calculator Python Script